ISSN 8755-6839

SCIENCE OF **TSUNAMI HAZARDS**

Journal of Tsunami Society International

Volume 35 **Number 1** **2016**

DETECTION OF TSUNAMI RADIATION AT ILLAPEL, CHILE ON 2015-9-16 BY REMOTE SENSING

Frank C Lin[1,*], Kingkarn Sookhanaphibarn[1], Worawat Choensawat[1], George Pararas-Carayannis[2]

[1]Multimedia Intelligent Technology Laboratory, School of Science and Technology, Bangkok University, Rama 4 Rd, Khlong Toei, Bangkok 10110, Thailand

[2]Tsunami Society International, Honolulu, Hawaii 96815, USA

ABSTRACT

We have detected the Tsunami Radiation generated by the 8.3 magnitude seaquake at Illapel, Chile on 2015-9-16 at the following wavelengths: 3.9 μm, 6.5 μm, 10.7 μm, and 13.3 μm. No radiation is detected at 0.63 μm, which is in the visible spectrum. The Tsunami Signals that we have observed did not decay within 44 minutes. From the satellite the Peru-Chilean Trench is visible in infrared space. In order to facilitate research in this field we attach the MATLAB code in an Appendix.

Keywords: *Tsunami Radiation, Tsunami Signal, Remote Sensing, Tsunami Decay, Illapel Chile*

**Corresponding author. Email: linbfrank@gmail.com. Tel/Fax: +662 612 4705*

1. INTRODUCTION

As reported by the USGS and others [USGS, 2015], on 16 September 2015 an earthquake with epicenter at 31.577° S, and 71.652 W., occurred at 19:54:33, Chile Standard Time (22:54:33 UTC), 46 km offshore from Illapel, Chile. Based on analysis of the moment tensor, the USGS determined that the nodal plane of this event had a strike of 4.0 deg., a dip of 19.0 deg., and that the seismic moment release was 3.2 x 10^{28} dyn-cm, corresponding to Moment Magnitude of Mw = 8.3. The initial quake lasted three minutes and was followed by several aftershocks greater than magnitude six. The Chilean government reported 13 deaths and 6 persons missing. The relatively minor damage and small loss of life caused by a quake of this magnitude and of the tsunami it generated, was largely due to low population density in the region and to the unique bathymetry and coastal geomorphology along this segment of the Chilean coastline.

The earthquake was caused by thrust faulting on the interface between the Nazca and the South American tectonic plates in Central Chile. As it has been postulated for Peru and Chile, the angle of subduction of the Nazca oceanic plate beneath South America is not uniform along the entire segment of the Peru-Chile Trench. Furthermore, the relatively narrow zone of subduction is affected by buoyancy forces of the bounding oceanic ridges and fractures and is characterized by shallow earthquakes that can generate destructive tsunamis of varied intensities (Pararas-Carayannis, 2012). Specifically at the latitude of this particular event, the Nazca plate is moving towards the east-northeast at a velocity of 74 mm/yr with respect to South America and begins subducting beneath the continent, 85 km to the west of the area which was affected by the 16 September 2015 earthquake. The size, location, depth and mechanism of this event in central Chile, are all consistent with its occurrence on the megathrust interface in this region. The anomalous, rupturing in opposing directions probably had a diminishing effect on tsunami generating efficiency.

As it was indicated for the 2011 Japan earthquake (Pararas-Carayannis, 2014), unusual clustering and chronological sequencing of aftershocks are indicative of segmented and gradual release of tectonic stress. For the event in Chile, the energy was also released gradually by separate events on adjacent faults and this may partially account for observations of different degrees of inundation along the Bay of Valparaiso and of the tsunami's directional approach as well as for the lesser, far-field tsunami impact (Pararas-Carayannis, report in prep.)

The area affected by the earthquake is estimated to have been about 230x100 km, or more concisely 23,000 sq. km. By comparison, the distance from Illapel to Santiago is approximately 230 km. The vastness of the quake-affected area had a bearing on the decay rate of the tsunami radiation signal, as we shall demonstrate. Preliminary evaluation of the source mechanism of tsunami generation associated with this earthquake - as inferred from geologic structure, rupturing process, seismic intensities, spatial distribution of aftershocks, energy release and fault plane solutions - indicates that heterogeneous crustal displacements took place along the entire length of the earthquake rupture (Pararas-Carayannis, report in prep.)

The tsunami impacted the entire Pacific region. Locally, preliminary post-disaster surveys in the vicinity of Valparaiso Bay, showed that the tsunami had a focused impact along certain locations in the Coquimbo coastal area, where maximum runup of up to 6 meters caused significant damage. Other impacted villages were Concon, Los Vilos and Tongoy, where the tsunami runup varied considerably ranging from less than 2 meters and up to 3-5 meters in certain locations. As reported by the USGS, the tsunami was recorded with the following maximum wave amplitudes in meters at these selected tide stations: 4.75 at Coquimbo, 1.78 at Valparaiso, 0.88 at Constitucion, 0.83 on Easter Island, 0.67 at Pago Pago, American Samoa; 0.15 at Quepos, Costa Rica; 0.56 on Isla Santa Cruz, Ecuador; 1.37 on NukuHiva, French Polynesia; 0.26 at Kushimoto, Japan; 0.37 at Puerto Angel, Mexico; 0.35 on Chatham Islands, New Zealand; 0.55 at La Punta, Peru; 0.44 at Shikotan, Russia; 0.34 at Ventura, California; and 0.90 at Hilo, Hawaii.

The map below shows the directivity of tectonic plate movements along the boundaries of the Nazca plate [Wikipedia, 2015].

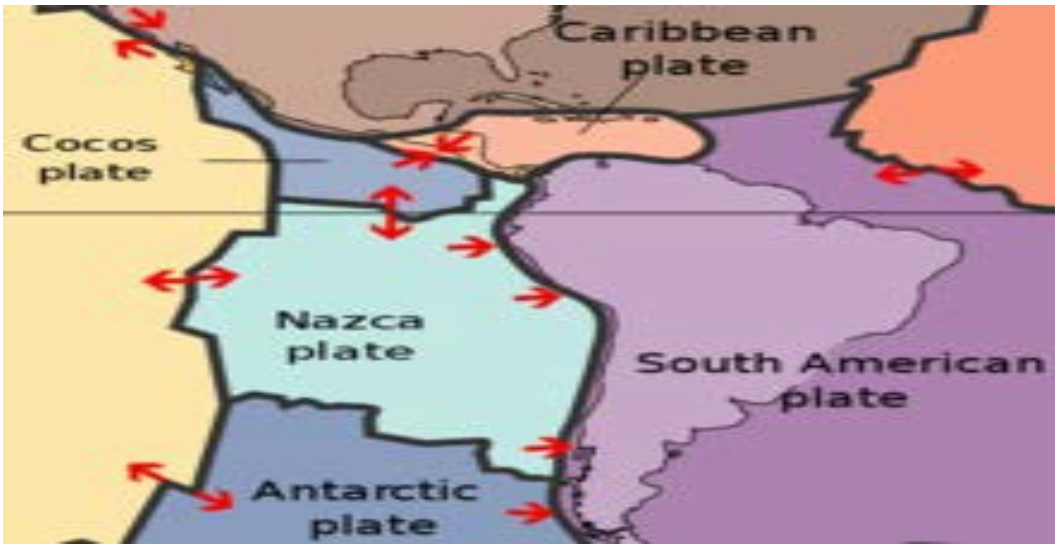

Fig.1: Tectonic motion of the Nazca plate

Generally, examination of earthquakes along the Nazca-South America convergence margin of Chile's northern end of the central seismic region are indicative of the complexity in the moment release, which can be correlated to structural variations within the subducting and overriding plates. The anomalous interactions affect crustal displacements and, therefore, the source characteristics of tsunamis that can be generated from large-scale, thrust and reverse thrust seismic events in the region - nucleated by offshore compressional earthquakes (Pararas-Carayannis, 2010)

2. THE SATELLITE

The GOES-13 (Geostationary Operational Environmental Satellites) is a geosynchronous satellite situated at 36,000 km above the equator at 75˚ W longitude. The GOES satellites are three- axis stabilized, giving the Imager and Sounder a continuous view of the Earth. The Imager has a total of 22 detectors split into three groups: 1) Eight visible detectors, 2) Seven primary infrared detectors, and 3) Seven redundant infrared detectors. Each of the 22 detectors is a member of one of five spectral channels. Although physically distinct, the five channels are optically overlaid. For GVAR (GOES Variable) the uplink bit rate is 2000 bps at a frequency of 2034 Mhz. The IR detector data segment contains the scan line data for the associated detector. This segment varies in length directly with the scan line, reaching a maximum nominal length of 52,360 bits (5236 pixels) for a 19.2˚ wide scan. [NASA, 2015]. The scan mirror positioning for both instruments is controlled by two servo motors, one for the north-south elevation angle (outer gimbal motor) and one for the east-west scanning azimuth angle (inner gimbal motor). Errors may occur in the detector response characteristics due to aging of and temperature variations in the instrument components. In addition, the IR detectors are subject to a low frequency random drift. Blackbody measurements are used to determine detector response characteristics, (specifically, gain and bias), based on an established relationship between blackbody temperature and equivalent target radiance as measured by each detector. The accuracy of the imager is 1 km for the visible detector and 4-8 km for the infrared detector.

In the following figure (Fig. 2) we show a satellite image taken by GOES-13 on 2015-9-16 at 23:08 UTC for the 10.7 μm channel

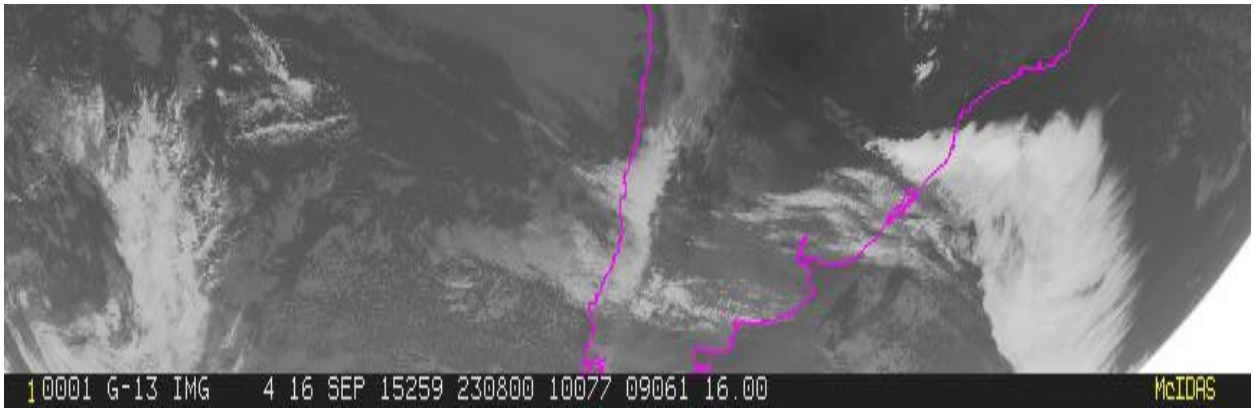

Fig.2: Goes-13 image for South America on 2015-9-16 at 23:08 UTC for the 10.7 μm channel

2. THE TSUNAMI RADIATION

In previous publications [Lin et al, 2010; Lin and Sookhanaphibarn, 2011; Lin et al., 2011; Lin et al., 2012; Lin et al., 2013; Lin et al., 2014, Lin et al, 2015] we have described the procedure by which a Signal Diagram can be extracted from the satellite image. Thus,

Algorithm 1:
begin
load($JPGfilename, Y_{tsunami}$, $X_{tsunami}$)

$imageDat$ = imread($JPGfilename$)

$rowDat$ = imageDat($Y_{tsunami}$; :)

$columnDat$ = imageDat(:;$X_{tsunami}$)
return($rowDat, columnDat$)
end

Here, $rowDat$ is the latitudinal Signal Diagram and $columnDat$ the longitudinal Signal Diagram. Y_t ; $X_{tsunami}$ are the coordinates of the earthquake epicenter, and $JPGfilename$ refers to the satellite image. To assist investigators who might wish to reproduce or extend our work we are posting the complete MATLAB code in the Appendix.

For channel 1 the Signal Diagram is given below:

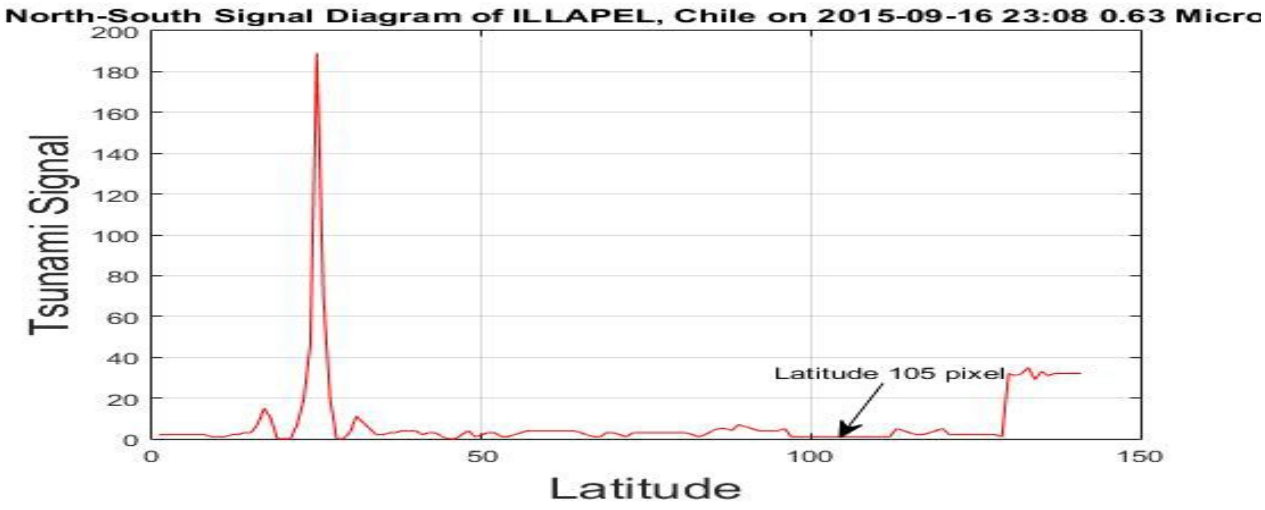

Fig.3: Longitudinal Signal Diagram on 2015-09-16 at 23:08 UTC for 0.63 µm

We observe that no signal was detected by GOES-13 at 23:08 UTC, which is 14 minutes after the 8.3 magnitude seaquake. This is due to the fact that the frequency 0.63 µm is in the visible spectrum, and the water molecules do not radiate at this frequency [Coudert *et al*., 2004; Coudert, 1997; Toth, 1991; Toth, 1993]. Had it been otherwise, we would have observed the entire sky painted in red! Our experimental measurement therefore confirms theoretical expectation.

In Fig. 4 we show the Signal Diagram for channel 2 at 3.9 μm:

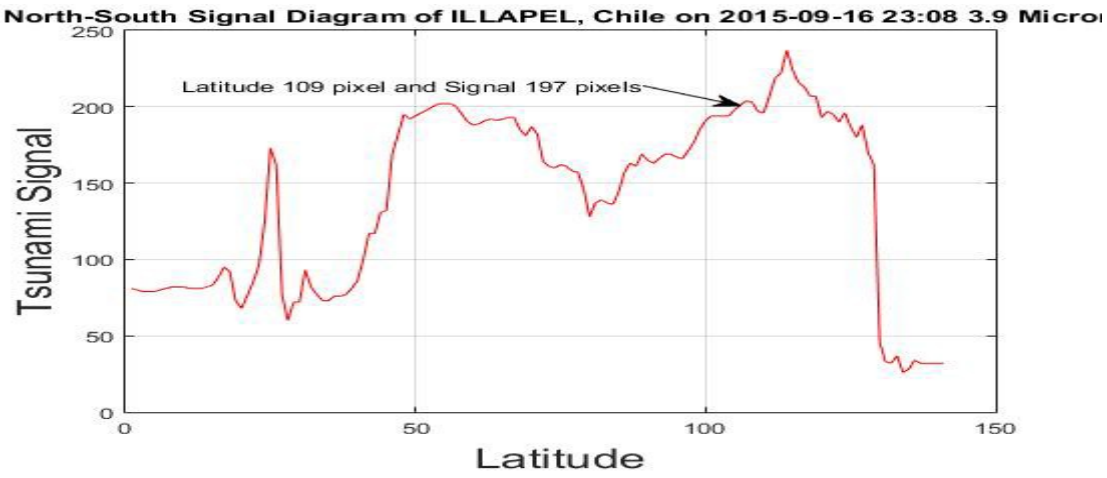

Fig.4: Longitudinal Signal Diagram on 2015-09-16 at 23:08 UTC for 3.9 μm

A Tsunami Signal of magnitude 197 pixels is observed. The intermediate infrared channel (IIR) at 3.9μm belongs to the IR-C band in the infrared spectrum. This band is used for tracking purposes by heat seeking missiles. In the presence of a tsunami, therefore, a missile might be misdirected from its target.

In Fig 5 we show the Signal Diagram for channel 3 at 6.5 μm:

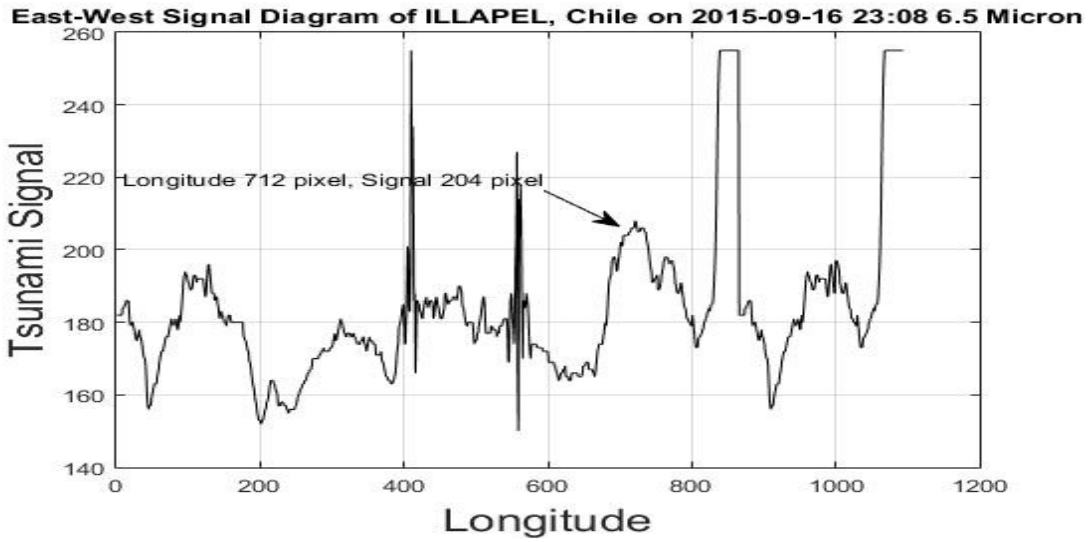

Fig.5: Latitudinal Signal Diagram on 2015-09-16 at 23:08 UTC for 6.5 μm

This is the Water Vapor channel which shows the amount of moisture in the air. As the moisture content of the air may vary greatly due to the action of wind, the tsunami signal may also fluctuate with time.

In Fig. 6 we show the Signal Diagram for channel 4 at 10.7 μm:

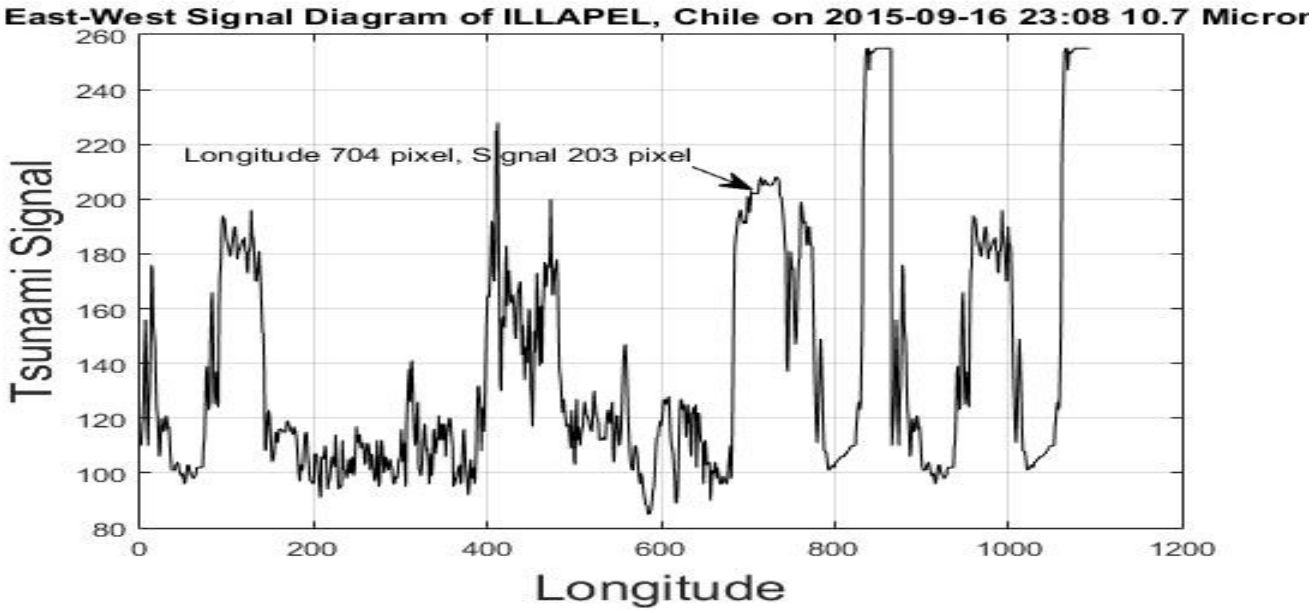

Fig.6: Latitudinal Signal Diagram on 2015-09-16 at 23:08 UTC for 10.7 μm

At this frequency, the Tsunami Signal is robust and we have utilized it in all of our previous investigations [Lin *et al*, 2010; Lin and Sookhanaphibarn, 2011; Lin *et al.*, 2011; Lin *et al.*, 2012; Lin *et al.*, 2013; Lin *et al.*, 2014, Lin *et al*, 2015]. The IR photon energy is between 0.001 and 1.7 eV.

This channel is the atmospheric window covered by detectors such as HgCdTe and microbolometers. Satellite images in this frequency region can be used to determine cloud heights and types, to calculate land and surface water temperatures, and to locate ocean surface features.

Finally, we show the Latitudinal Signal Diagram for channel 5 at 13.3 μm:

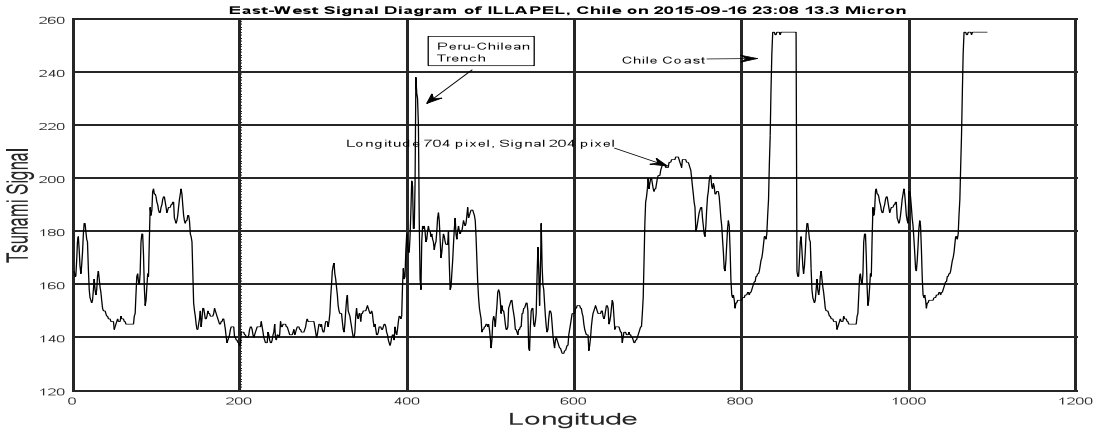

Fig.7: Latitudinal Signal Diagram on 2015-09-16 at 23:08 UTC for 13.3 μm

This Signal Diagram, which represents a slice across the satellite image along the latitude of the seaquake event from West to East, has two interesting features not so evident in the longitudinal Signal Diagrams: 1) the Tsunami Signal is very broad, extending approximately 25 pixels in width (corresponding to a terrestrial distance of about 100 km); 2) The Chilean coastline is clearly delineated, as pointed to by an arrow. Also of interest is that in all Latitudinal Signal Diagrams the enhanced radiation on the *subduction zone* from pixel = 400 up to 700 pixels is exhibited, as compared with the radiation emanating from the Pacific Ocean for pixel < 400 pixels. The Peru-Chilean trench is demarcated by a strong peak as pointed to by an arrow.

We summarize the above result in the following table: In this table we have also included the data measured at 23:38 UTC for comparison.

Table 1: Table of Tsunami Signals (S_1, S_2)*

channel	**Image time 23:08 S_1 pixels**	**Image time 23:38 S_2**	**Mode**	**Remark**
1. 0.63 μm	0.0	0.0	N/A	Cloud and surface features
2. 3.9 μm	197	194	Overtones, Combinatio	Low cloud, fog, fire
3. 6.5μm	204	200	V_2	WV
4. 10.7μm	202	201	R,L1,L2	Surface/Cloud top temperature
5. 13.3μm	206	201	R,L1,L2	Cloud heights

*The Longitudinal (North-South) Signal Diagrams are used for these measurements

The excitation of the water molecule can occur after multiple collisions. For a detailed analysis it is necessary to perform a quantum mechanical calculation for the transition probability of water molecule from the ground state to the excited state. Since the number of molecules participating in this event is of the order of 10^{36} [Lin et al, 2015], we expect that the radiation will be significant.

In previous work we have assumed that the tsunami eye extends to an area 10 km * 10 km and that the tsunami signal will subside within half an hour. Here, however, we have a case where the tsunami eye is 230 km * 100 km and the signal lasts for over an hour. We speculate that an observer navigating in the vicinity of the tsunami eye will be able to observe a gigantic cacophony of '*Son et lumière'* show lasting over an hour, provided the observer wears a pair of infrared goggles. Indeed, the radiation will be observable in outer space, presumably by aliens.

On the molecular level, this radiation with wavelength 13.3 μm (751.9 cm^{-1}) corresponds to the rotational quantum level transition from (6 4 3) to the ground state (0 0 0) measured spectroscopically by Toth et al, who obtained a result of 756.7 cm^{-1}.[Toth,1991]. The discrepancy may be accounted for by the Coriolius Effect, the Centrifugal Effect, and above all, the Doppler Effect due to the high velocity of the molecules. Both the satellite measurement and the spectroscopic measurement are subject to experimental errors. For transitions at the other frequencies refer to [Lin et al; 2015]. The mode designates the type of motion executed by the water molecule in its excited state before transition to the ground state by emitting a photon.

3. CONCLUSION

We hypothesize that a seaquake with magnitude greater than 7.0 will generate a tsunami accompanied by multispectral radiation in the infrared domain. Previous studies [Lin et al, 2010; Lin and Sookhanaphibarn, 2011; Lin et al., 2011; Lin et al., 2012; Lin et al., 2013; Lin et al., 2014, Lin et al, 2015] confirm that this is indeed the case for Banda Aceh (2004), Tohoku (2011), N. Sumatra (2011), and Sulangan (2012). Two cases, Bio-Bio (2010) and Ofunato (2012) have issues that are not definitively resolved, but do not constitute counter-examples. The present investigation reaffirms the validity of our hypotheses. We detected infrared radiation at the following wavelengths: 3.9 μm, 6.5 μm, 10.7 μm, and 13.3 μm. No radiation is detected at 0.63 μm, which is in the visible spectrum. The Tsunami Signals that we have observed did not decay within 44 minutes. This is probably related to the exceptionally huge size of the tsunami eye. The radiation at 13.3 μm corresponds to the rotational quantum level transition from (6 4 3) to the ground state (0 0 0). We note that the elevated temperature and the high speed of the molecules in a tsunami are energetically capable of stimulating the molecules to excited quantum energy levels by collisions.

REFERENCES

[USGS,2015] http://earthquake.usgs.gov/earthquakes/eventpage/us20003k7a#general_summary . Retrieved September 16, 2015

[Wikipedia,2015] https://en.wikipedia.org/wiki/2015_Illapel_earthquake

[NASA,2015] http://goes.gsfc.nasa.gov/text/GVARRDL98.pdf

Coudert, L.H., 1994. Analysis of the Rotational Levels of Water and Determination of the Potential Energy Function for the Bending ν2 Mode: J. of Mol. Spectroscopy 165, pp.406-425.

Coudert, L.H., 1997. Analysis of the Line Positions and Line Intensities in the ν2 Band of the Water Molecule: J. of Mol. Spectroscopy 181, pp.246-273

Coudert, L.H., O.Pirali, M.Vervloet, R.Languetin and C.Camy-Peyret, 2004. The eight first vibrational states of the water molecule: measurement and analysis. J. of Molecular Spectroscopy 228, pp. 471-498.

Lanquetin, R., L.H.Coudert and C.Camy-Peyret, 1999. High-Lying Rotational Levels of Water: Comparison of Calculated and Experimental Energy Levels for (0 0 0) and (0 1 0) up to J=25 and 21. J. of Mol. Spectroscopy 195, 54-67.

Lanquetin, R., L.H.Coudert and C.Camy-Peyret, 2001. High-Lying Rotational Levels of Water: An Analysis of the Energy Levels of the Five Vibrational States: J. of Mol. Spectroscopy 206, 83- 103.

Lin F.C., K. Na Nakornphanom, K. Sookhanaphibarn, and C. Lursinsap, 2010."A New Paradigm for Detecting Tsunamis by Remote Sensing"; International Journal of Geoinformatics, Vol.6, No.1, March 2010, pp.19-30.

Lin F.C. and K. Sookhanaphibarn, 2011. Representation of Tsunamis in Generalized Hyperspace: Proceedings of the IEEE International Geoscience and Remote Sensing Symposium (IGARSS'11), Sendai/Vancouver, July 21, 2011. pp. 4355-4358.

Lin F.C., W. Zhu and K. Sookhanaphibarn, 2011. Observation of Tsunami Radiation at Tohoku by Remote Sensing, Science of Tsunami Hazards, Vol.30, No.4,Honolulu, HI, December 2011, pp. 223-232.

Lin, F.C., W. Zhu and K. Sookhanaphibarn, 2012. A Detail Analysis of the Tohoku Tsunami by Remote Sensing, Proceedings of the IEEE International Geoscience and Remote Sensing Symposium (IGARSS'12), Munich, Germany, pp.1166-1169.

Lin. F.C., W. Zhu, K. Sookhanaphibarn and P. Silapasuphakornwong, 2013. REMOTE:-A Satellite Based Tsunami Early Warning Detection System, Proceedings of the IEEE International Geoscience and Remote Sensing Symposium (IGARSS' 13), Melbourne, Australia, pp. 3694- 3697.

Lin, F.C., K. Sookhanaphibarn, V. Sa-yakanit and G. Pararas-Carayannis, 2014. REMOTE: Reconnaissance & Monitoring of Tsunami Events, Science of Tsunami Hazards, Vol.33, No.2, pp.86-111

Lin, F.C., K.Sookhanaphibarn, W. Choensawat and G. Pararas-Carayannis: On the Frequency Spectrum of Tsunami Radiation, Science of Tsunami Hazards, Vol.34, No.3, pp.34

Martin, W.C. and W.L.Wiese, 1996.Atomic, Molecular and Optical Physics Handbook, G.W.R.Drake, Ed., AIP Press, Woodbury, N.Y.

Pararas-Carayannis, G., 2010. The earthquake and tsunami of 27 february 2010 in Chile – Evaluation of Source Mechanism and of Near and Far-field Tsunami Effects. Science of Tsunami Hazards, *Vol. 29, No. 2, pp 96 - 126 (2010)*

Pararas-Carayannis, G., 2012. Geodynamics of Nazca ridge's oblique subduction and migration - implications for tsunami generation along central and southern Peru: Earthquake and Tsunami of 23 June 2001. Science of Tsunami Hazards, Vol 31, No. 2, pp. 129-153, 2012

Pararas-Carayannis, G., 2013. "The Great Tohoku-Oki Earthquake and Tsunami of March 11, 2011 in Japan: A Critical Review and Evaluation of the Tsunami Source Mechanism," Pure and Applied Geophysics, pp. 1-22.

Tennyson, J., N.F. Zobov, R. Williamson, O.L. Polyansky, P.F. Bernath, 2001. Experimental energy levels of the water molecule. Journal of Physical and Chemical Reference Data, 30 (3). pp. 735- 831.

Toth, R. A., 1991. ν2 band of H216O: line strengths and transition frequencies. J. Opt. Soc. Am. B, Vol.8, No.11, November 1991, pp.2236-2255.

Toth, Robert A., 1993. 2ν2 – ν2 and 2ν2 bands of H216O, H217O and H218O: Line Positions and Strength: J. Opt. Soc. Am. B, Vol.10, No.9, September 1993, pp. 1526-1544.

APPENDIX

```
%mainTsunamiDetection6.m
% Clear paramethers and close all windows
%clear
clc
close all
warning('off','MATLAB:dispatcher:InexactCaseMatch');
% INPUT FILES
%display(' Please enter TITLE, such as 'TOHOKU 2011-3-11 06:30 UTC');
%TITLE = input('Please enter TITLE of this project in quotes;e.g. TOHOKU DATE
of image,TIME UTC:  ');
JPGfilename= input('input image name e.g."COUNTRY_GOES_IMAGE.jpg: "  ');
%display(' Please enter JPG filename for satellite image:'};
%display('  ');
%display('  ');
REFfilename= 'Country_mainshock_ref.tex';
%REFfilename=input('INPUT the file for three reference points to be read into
MATLAB:', 's');
%display(' Please enter latitute & longitude of three reference points and
%their pixel values:');
% Note
% Range for Deletion = 75:220

% Main Procedure
fopen(JPGfilename);
ReadJPG( JPGfilename );
%clear command window;
[X_tsunami, Y_tsunami]=calculatePixelForEarthquake6(REFfilename);
rowDat =
extractRowDatMainshock6(JPGfilename,round(Y_tsunami),round(X_tsunami));
display('Now write TITLE,save signal diagram,workspace,and press enter to call
WAVEMENU:');
pause;
wavemenu;
% Use 1D signal, import signal, and do Analysis:
% This is the end of the Program

function [X_tsunami, Y_tsunami]=calculatePixelForEarthquake6(~)
%calculatePixelForEarthquake6.m
fid = fopen('Country_mainshock_ref.tex');
tline = fgetl(fid);
display('Enter the pixel values of A and B and the earthquake position:');
display('NOTE:The southern or Western hemisphere,longitude and latitude may be
negative.');
disp('ACHTUNG. For A,B and earthquake epicenter --');
disp('all latitudes and longitudes must have the same sign.');
beep on;
disp('In northern hemispere, CHOOSE lat A < lat of epicenter and lat B > lat
of epic: ');
```

```
disp('Choose long A < long of epic and long B > long of epic.');
disp('Ditto in southern hemisphere. lat and long of A must be less than those
of epicenter and B.');
disp('A and B must enclose earthquake epicenter.');
display(datestr(now));
pause(5);
beep off;
while ischar(tline)
    tline = fgetl(fid);
    if (tline(1)==' ')
        display(' ');
    elseif (~isempty(strfind(tline,'RefA_Xco')))
        RefA_Xco=str2num(tline(strfind(tline,'=')+1:length(tline)));
    elseif (~isempty(strfind(tline,'RefA_Yco')))
        RefA_Yco=str2num(tline(strfind(tline,'=')+1:length(tline)));
    elseif (~isempty(strfind(tline,'RefB_Xco')))
        RefB_Xco=str2num(tline(strfind(tline,'=')+1:length(tline)));
    elseif (~isempty(strfind(tline,'RefB_Yco')))
        RefB_Yco=str2num(tline(strfind(tline,'=')+1:length(tline)));
 %   elseif (~isempty(strfind(tline,'RefC_Xco')))
 %       RefC_Xco=str2num(tline(strfind(tline,'=')+1:length(tline)));
 %   elseif (~isempty(strfind(tline,'RefC_Yco')))
 %       RefC_Yco=str2num(tline(strfind(tline,'=')+1:length(tline)));
    elseif (~isempty(strfind(tline,'RefA_Lat')))
        RefA_Lat=str2num(tline(strfind(tline,'=')+1:length(tline)));
    elseif (~isempty(strfind(tline,'RefA_Lon')))
        RefA_Lon=str2num(tline(strfind(tline,'=')+1:length(tline)));
    elseif (~isempty(strfind(tline,'RefB_Lat')))
        RefB_Lat=str2num(tline(strfind(tline,'=')+1:length(tline)));
    elseif (~isempty(strfind(tline,'RefB_Lon')))
        RefB_Lon=str2num(tline(strfind(tline,'=')+1:length(tline)));
 %   elseif (~isempty(strfind(tline,'RefC_Lat')))
 %       RefC_Lat=str2num(tline(strfind(tline,'=')+1:length(tline)));
 %   elseif (~isempty(strfind(tline,'RefC_Lon')))
 %       RefC_Lon=str2num(tline(strfind(tline,'=')+1:length(tline)));
    elseif (~isempty(strfind(tline,'Lat')))
        Lat=str2num(tline(strfind(tline,'=')+1:length(tline)));
    elseif (~isempty(strfind(tline,'Lon')))
        Lon=str2num(tline(strfind(tline,'=')+1:length(tline)));
    else disp(' ');
    end
end
fclose(fid);
%NOTE! the longitude increses from east to westin the eastern hemisphere,
while the pixel value
%decreases from east to west:
%NOTE: the latitude increases from north to south in the northern hemisphere;
while the pixel value
%decreases from north to south.
```

```
%The latitide in the southern hemisphere is negatine;
%The longitude in the western hemiphere is negative.
reply = input('Are the geodectics all in the northern hemisphere? (y/n): ',
's');

if strcmp(reply,'y')
  disp(reply)
end
if reply == 'y' %true
if Lon > RefA_Lon
    X_tsunami=abs(abs((abs(Lon-RefA_Lon)/abs(RefB_Lon-RefA_Lon))*abs(RefB_Xco-
RefA_Xco)+abs(RefA_Xco)));%end%longitude pix decreases from C
end
if Lat > RefA_Lat
    Dgeo=abs(Lat - RefA_Lat);
    A2Bgeo=abs(RefA_Lat-RefB_Lat);
    A2Bpix=abs(RefA_Yco-RefB_Yco);
    Dpix=A2Bpix*Dgeo/A2Bgeo;
    Y_tsunami=RefA_Yco-abs(Dpix);
end
 % Y_tsunami=abs(abs((abs(Lat-RefA_Lat)/abs(RefB_Lat-RefA_Lat))*abs(RefB_Yco-
RefA_Yco)+abs(RefA_Yco)));%lat pixel increases from A

if Lat < RefA_Lat
    Dgeo=abs(Lat - RefA_Lat);
    A2Bgeo=abs(RefA_Lat-RefB_Lat);
    A2Bpix=abs(RefA_Yco-RefB_Yco);
    Dpix=A2Bpix*Dgeo/A2Bgeo;
    Y_tsunami=RefA_Yco+abs(Dpix);
%Y_tsunami=abs(abs((abs(Lat-RefA_Lat)/abs(RefB_Lat-RefA_Lat))*abs(RefB_Yco-
RefA_Yco)-abs(RefA_Yco)));%lat pixel decreases from A
end

if Lon < RefA_Lon
      Dgeo=abs(Lon - RefA_Lon);
    A2Bgeo=abs(RefA_Lon-RefB_Lon);
    A2Bpix=abs(RefA_Xco-RefB_Xco);
    Dpix=A2Bpix*Dgeo/A2Bgeo;
    X_tsunami=RefA_Xco-abs(Dpix);
 %X_tsunami=abs(abs((abs(Lon-RefA_Lon)/abs(RefB_Lon-RefA_Lon))*abs(RefB_Xco-
RefA_Xco)-abs(RefA_Xco)));
end

if reply == 'n' % false
    if Lon > RefA_Lon
         Dgeo=abs(Lon - RefA_Lon);
    A2Bgeo=abs(RefA_Lon-RefB_Lon);
    A2Bpix=abs(RefA_Xco-RefB_Xco);
    Dpix=A2Bpix*Dgeo/A2Bgeo;
    X_tsunami=RefA_Xco+abs(Dpix);
```

```
%    X_tsunami=abs(abs((abs(Lon-RefA_Lon)/abs(RefB_Lon-
RefA_Lon))*abs(RefB_Xco-RefA_Xco)+abs(RefA_Xco)));%end%longitude pix decreases
from C
    end
    if Lat > RefA_Lat
    Dgeo=abs(Lat - RefA_Lat);
    A2Bgeo=abs(RefA_Lat-RefB_Lat);
    A2Bpix=abs(RefA_Yco-RefB_Yco);
    Dpix=A2Bpix*Dgeo/A2Bgeo;
    Y_tsunami=RefA_Yco-abs(Dpix);
    end
    % Y_tsunami=abs(abs((abs(Lat-RefA_Lat)/abs(RefB_Lat-
RefA_Lat))*abs(RefB_Yco-RefA_Yco)+abs(RefA_Yco)));%lat pixel increases from A

if Lat < RefA_Lat
    Dgeo=abs(Lat - RefA_Lat);
    A2Bgeo=abs(RefA_Lat-RefB_Lat);
    A2Bpix=abs(RefA_Yco-RefB_Yco);
    Dpix=A2Bpix*Dgeo/A2Bgeo;
    Y_tsunami=RefA_Yco+abs(Dpix);
%Y_tsunami=abs(abs((abs(Lat-RefA_Lat)/abs(RefB_Lat-RefA_Lat))*abs(RefB_Yco-
RefA_Yco)-abs(RefA_Yco)));%lat pixel decreases from A
end

if Lon < RefA_Lon
      Dgeo=abs(Lon - RefA_Lon);
    A2Bgeo=abs(RefA_Lon-RefB_Lon);
    A2Bpix=abs(RefA_Xco-RefB_Xco);
    Dpix=A2Bpix*Dgeo/A2Bgeo;
    X_tsunami=RefA_Xco-abs(Dpix);
 %X_tsunami=abs(abs((abs(Lon-RefA_Lon)/abs(RefB_Lon-RefA_Lon))*abs(RefB_Xco-
RefA_Xco)-abs(RefA_Xco)));
end
end

display(X_tsunami);

display(Y_tsunami);

pause(5);

end

function rowDat = extractRowDatMainShock6(JPGfilename,Y_tsunami,X_tsunami)
%load(JPGfilename);
imageFile=imread(JPGfilename);

im = imageFile;
rowDat = im(Y_tsunami,:);
columnDat = im(:,X_tsunami);
```

```
pause on;

pause(2);
%plot(1:length(rowDat),rowDat);
x=1:length(rowDat);
y=1:length(columnDat);
figure, grid on;
title('East-West Signal Diagram');
plot(x,rowDat,'k');
ylabel('Tsunami Signal','FontSize',18);
xlabel('Longitude','FontSize',18);
%PLOTTOOLS;

low=input('Input the range of X-pixels for deletion (starting point) :');

u=input('Input the range of X-pixels for deletion (ending point) :');
pause(1);
rowDat(low:u)=[];
%legend(TITLE);
x=1:length(rowDat);
figure, plot(x,rowDat,'k');
ylabel('Tsunami Signal','FontSize',18);
xlabel('Longitude','FontSize',18);
grid;
pause(10);

disp('Now plot columnDat.');
pause(10);
figure, title('North-South Signal Diagram');
plot(y,columnDat,'r');
grid;
ylabel('Tsunami Signal','FontSize',18);
xlabel('Latitude','FontSize',18);
%disp('Press Enter to continue:');
%low=input('Input the range of X-pixels for deletion (starting point) :');
%u=input('Input the range of X-pixels for deletion (ending point) :');
pause(3);
%close(h);
disp('EW Tsunami Signal = ');
disp(rowDat);
disp('NS Tsunami Signal = ');
disp(columnDat);
%pause off;
%saveFile=strrep(rowDat,'.jpg','.mat');
%eval(['save ' saveFile ' rowDat']);
disp('Y value of earthquake:Y_tsunami= ');disp(Y_tsunami);
disp('X value of earthquake:X_tsunami= ');disp(X_tsunami);
```

```
S=max(rowDat);
disp('Max value of EW signal is:');disp(S);

%Goto wavemenu for Signal Diagram importing signal from workspace, using 1D
wavelet
%
%figure;
%plot(rowDat); hold on;
%GRID;
%text(xLoc,double(rowDat(xLoc))+20,'\leftarrow ','FontSize',18);
%Title;
hold off;
pause(5);
%figure;
%plot(columnDat);  hold on;
%GRID;
%ylabel('Tsunami Signal','FontSize',18);
%xlabel('Latitude','FontSize',18);
hold off;
display('wavemenu starts;USE IMPORT "ANS" FROM WORKSPACE FOR SIGNAL. ');
pause(3);
%USE IMPORT "ANS" FROM WORKSPACE FOR SIGNAL
%Copyright:Kingkarn Sookhanaphibarn & Frank C Lin
end


function ReadJPG( JPGfilename )
%Read a JPG file into MATLAB
a=imread(JPGfilename,'jpg');
imtool(a);
end
```